Chapter 9

Optical Coherence Tomography – Applications in Non-Destructive Testing and Evaluation

Alexandra Nemeth, Günther Hannesschläger, Elisabeth Leiss-Holzinger, Karin Wiesauer and Michael Leitner

Additional information is available at the end of the chapter

http://dx.doi.org/10.5772/53960

1. Introduction

The field of non-destructive testing and evaluation (NDTE) comprises many different techniques and approaches. Over the past few decades there have been tremendous advances in NDTE technology, allowing researchers and engineers to tackle problems in many scientific and industrial fields. However, techniques enabling a fast, contactless, non-invasive, and high-resolution imaging of subsurface features at a level of only a few microns are still scarce.

One technology fulfilling all of these requirements is optical coherence tomography (OCT) [1]. OCT is a purely optical, non-destructive, non-invasive, and contactless high resolution imaging method, which allows the acquisition of one-, two- or three-dimensional depth resolved image data of sub-surface regions in situ and in real time. The outstanding depth resolution of OCT can be as good as or even better than one micrometer [2]. OCT is an already well-established diagnostics technique for biomedicine and advanced life science applications. Emerging originally from the field of ophthalmology, OCT has also received a lot of interest in other biomedical areas like e.g. dentistry [3], dermatology [4], cardiology [5], and developmental biology [6].

The potential of OCT to become an outstanding imaging technique also outside the area of biomedicine has been recognized already within the first years after its invention [7,8]. However, only a few groups applied the technology to material related problems, and therefore the interest for this field of research has increased slowly [9–12]. A comprehensive review on OCT applications outside biomedicine was published by Stifter in 2007 [13].

Since then OCT has received increasing attention as a novel tool for NDTE, with more and more research groups being engaged in further exploring possible applications of OCT. Recent examples include, among many others, the measurement of layer thickness in multi-layered foils [14] or pharmaceutical tablets [15], the characterization of laser-drilled holes and micro-machined devices [16], organic solar cells [17], paper [18], or printed electronics products [19], applications in food [20] and polymer sciences [21], and the conservation of artwork [22].

This chapter will give a short overview on the technique of OCT, provide a brief overview on the historical development of OCT for non-destructive testing, and describe some of the most recent applications in this field.

2. Optical coherence tomography

OCT is based on the physical phenomenon of white light interferometry (WLI) and employs special light sources with high spatial but low temporal coherence (i.e., a large bandwidth spectrum), like e.g. superluminescent diodes, or femtosecond or supercontinuum lasers. Such sources have coherence lengths in the range of only several microns. In an interferometric detection system such a short coherence length acts like a temporal filter regarding the arrival times of the back-scattered photons. For currently used low coherence light sources the coherence length generally lies in the region of 1-15 μm, enabling an excellent axial (depth) resolution with OCT [2]. Due to the interferometric detection scheme OCT is well suited to image layered and micro-structured samples. The image contrast is due to inhomogeneities in the refractive index of the sample material, and thus, OCT provides complementary information to other high resolution imaging techniques like ultrasound, X-ray computed tomography (CT), and magnetic resonance imaging (MRI).

The nomenclature in OCT is analogous to the one used in ultrasound tomography. Single depth scans and cross-sections are classified as A- and B-scans, respectively. When imaging at a constant depth, it is possible to acquire the so-called en-face images or C-scans. The image plane of C-scans is perpendicular to the one of B-scans and has the familiar orientation of conventional microscopy images. An M-scan describes the acquisition of consecutive A-scans at one constant lateral position. In this case one dimension in the 2D image represents the progress in time.

2.1. Resolution

In comparison to other high resolution microscopic techniques, like e.g. confocal microscopy, OCT has the advantage that axial and lateral resolutions are decoupled. Therefore the imaging optics can be located away from the sample without penalizing the axial resolution. The axial resolution is limited by the center wavelength and the bandwidth of the optical light source, and is generally defined as one half of the coherence length l_c:

http://dx.doi.org/10.5772/53960

$$\Delta z = \frac{l_c}{2} = K \frac{\lambda_c^2}{\Delta\lambda}. \tag{1}$$

Here K denotes a constant factor (0.44 for an optical source with Gaussian spectral distribution), and λ_c and $\Delta\lambda$ describe the center wavelength and full width at half maximum (FWHM) bandwidth of the source, respectively.

The lateral resolution is solely determined by the probe optics and can be calculated over

$$\Delta x = 0.61 \frac{\lambda}{NA} \tag{2}$$

where NA is the numerical aperture of the imaging optics.

2.2. Spectral range and light sources

In OCT the sample is commonly illuminated with light in the near infrared (NIR). The choice of the right light source is crucial since it determines on the one hand the axial resolution and on the other hand the penetration depth. Light sources used in OCT should have very high spatial but very low temporal coherence (i.e. a large spectral bandwidth) and provide a smooth Gaussian shaped spectrum. In this way axial resolutions in the range of one micrometer can be achieved.

The penetration depth is determined by the attenuation characteristics of the sample, which can be described by the Beer-Lambert law

$$I_D(\lambda, z) = I_0 R_z \exp\left\{-2\int_0^z \mu_{att}(\lambda, z')dz'\right\} \tag{3}$$

where I_D describes the intensity measured at the detector, I_0 the initial intensity, R_z the reflection coefficient at depth z, and μ_{att} the attenuation coefficient. The attenuation coefficient μ_{att} is the sum of the scattering and the absorption coefficients, μ_{sca} and μ_{abs}, respectively, which are both functions of the wavelength λ. Consequently, the penetration depth is strongly dependent on the wavelength range used for the imaging process, since this determines the absorption and scattering of the light. With the right choice of the light source penetration depths of several millimeters can be achieved.

Historically the most important application for OCT is ophthalmology. Therefore a great part of the commercially available OCT systems are designed towards this specific application and comprise light sources centered around 800 nm, where absorption due to water is low. For many non-ophthalmic applications, however, it has been shown that imaging at different center wavelengths might be advantageous [13]. Promising spectral regions are located around 1300 nm and 1550 nm. Here scattering is reduced for many samples and the penetration depth is drastically increased. Anyway, the technique of OCT is applicable on a vast variety of materials, and basically for every application the most suitable spectral range has to be determined.

The three types of light sources mostly used in OCT are superluminescence diodes, femtosecond lasers, and supercontinuum laser sources. Since superluminescence diodes are rather cheap, provide nicely shaped Gaussian spectra, and are available at many different center wavelengths, they are the most popular kind of light source for OCT. However, the FWHM bandwidth of superluminescence diodes is limited to ≈ 100 nm, which constrains the axial resolution to several micrometers. Femtosecond laser sources offer higher bandwidths (typically up to ≈ 200 nm) and increased optical power, but are relatively expensive. Supercontinuum laser sources can cover a spectrum ranging from around 400 nm to 2400 nm, allowing for the acquisition of ultra-high resolution images.

2.3. Image acquisition and detection schemes

OCT is an interferometric approach, in which the depth-resolved information can be assessed by different means. In all approaches the probing beam is focused into the object and photons are back-scattered from different sample structures like interfaces, impurities, pores or cells. Only single scattered photons contribute to the useful signal, and by comparing their arrival times with a reference light beam a depth scan is obtained. Reconstruction of depth resolved cross sections (2D images) or volumes (3D images) is performed by scanning the probing beam laterally across the sample with the aid of galvanometer mirrors and subsequent acquisition of depth scans at adjacent lateral positions.

The depth resolved OCT signal can be acquired either in the time-domain or the spectral-domain, with the latter approach offering advantages in terms of imaging speed and sensitivity, enabling video rate imaging [23] and in-line applications [14]. On the other hand, the time-domain approach permits dynamic focusing and shows a constant sensitivity over the whole depth range.

In time-domain OCT the length of the reference arm in the interferometer is scanned over several millimeters while the sample is kept static. Due to the interferometric detection scheme and the short coherence length of the used light sources, a signal is detected only if the photons reflected from both interferometer arms have travelled the same optical distance to the photodetector. Otherwise only noise is detected. Obviously, the mechanical movement of the reference mirror is rather time consuming and may lead to mechanical instabilities and noise.

One way to speed up the image acquisition process is to use the so-called Fourier-domain OCT approach. Here the reference mirror is fixed and the light coming from both reference and object is detected in a spectrally resolved way. This can either be done in parallel (spectral-domain) by using a dispersing element and a CCD or CMOS camera, or sequentially by scanning a narrow laser line over a broad spectral region (swept-source OCT). Whatever the approach, in Fourier-domain OCT the depth information is encoded in a cosinusoidal modulation of the acquired spectrum and can be accessed by applying an inverse Fourier transform. With state-of-the-art cameras or swept laser sources A-scan rates of several hundred kHz can be achieved.

A schematic of a spectral-domain OCT system (left), and a photograph of an industrial OCT system, as developed in the labs at RECENDT (right), are depicted in Figure 1.

http://dx.doi.org/10.5772/53960

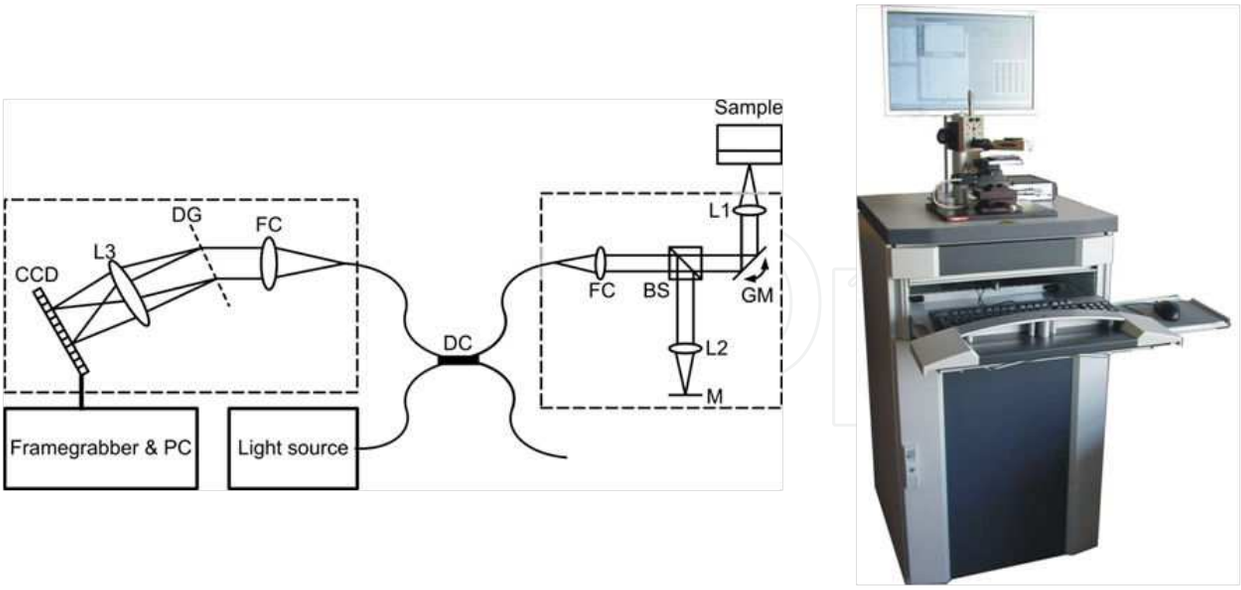

Figure 1. Left: Schematic of a spectral-domain OCT system. The dashed boxes represent portable and independent modules. DC – directional coupler; FC – fibre coupler; BS – beamsplitter; (G)M – (galvanometer) mirror; LX – lens; DG – diffraction grating. Right: Photograph of a spectral-domain OCT system developed at RECENDT.

3. Applications of OCT in non-destructive testing

OCT can provide both quantitative and qualitative information. The former includes e.g. the thickness of layers, or the size and distribution of pores, fibers or cells. With the aid of state-of-the-art image processing tools it is possible to automatically analyze sample features. Qualitative information is obtained through the visual inspection of the acquired images. Features like surfaces, impurities or cells can easily be detected and give rapid indications on the condition of the sample, providing important information to scientists or technicians.

Besides sample information based on pure reflectivity, it is also possible to take advantage of other types of contrast like birefringence for the detection of stress and strain (polarization-sensitive OCT) [12], the direction and velocity of fluids (Doppler OCT) [24], and spectral characteristics (spectroscopic or differential absorption OCT) [25].

Generally, information on the sample under investigation by means of OCT can be acquired under three different conditions: (i) with a lab based system assembled on an optical bench, (ii) with a desktop system (e.g. a commercially available device or a prototype system like in Figure 1), or (iii) directly at a production site in an industrial environment. Therefore, for each application the right system has to be chosen.

Lab-based systems have the most degrees of freedom, since different components like appropriate light sources, scanners, and detection devices can easily be connected in order to enable a rapid investigation of the sample. The drawback of such systems is that they are confined to the optical bench where all devices are assembled.

Nowadays there already exist several companies and research centers offering commercially available OCT systems or prototypes, respectively, which aim at applications outside the medical sector and the common optics laboratory. Generally, in such OCT devices all the necessary components, mostly except the computer, are embedded in one single casing. Such systems are ideal for test measurements and to analyze many kinds of samples. However, desktop systems offer little degrees of freedom, albeit several suppliers offer the possibility to built custom-inspired systems.

In some cases there is the need to tailor OCT systems towards one particular application. In biomedical imaging (e.g. ophthalmology, dermatology) this is already common practice. In the field of NDTE, however, there is still a quest for the "killer application", which would trigger the development of commercially available OCT systems tailored towards the investigation of one particular kind of sample. Therefore, so far most of the OCT systems used for the characterization of processes or specimens at industrial sites are specially designed prototypes, which hence are also still quite expensive. Recently one promising application coming up was the in-line-characterization of multi-layered foils directly at the production site [14].

The remainder of this chapter is now dedicated to the discussion of some recent applications of OCT in the field of non-destructive testing.

3.1. Characterization of multi-layered foils

Multi-layered plastic foils are commonly employed in the packaging industry to preserve the content from environmental influences. In food packaging, for example, different layers fulfill different purposes, such as protecting the interior from oxygen or providing good vapor permeability from the inside out. The production process of multi-layered foils at blown film extrusion lines typically comprises only one step. Especially in the case of barrier layers it is very important to guarantee the right layer thickness. The material used for such barrier layers is expensive, and therefore any material used in excess turns the production less cost-effective. On the other hand, if the layer is too thin the specifications might not be met, turning the foil useless. In order to ensure already during the production process that the final product matches the specifications, an in-line quality control is required. The parameters that need to be monitored in-line include the thickness and homogeneity of the individual layers and possible inclusions of air or impurities. A method to perform this task has to be non-destructive, fast, and must provide the ability to reveal the internal structure of (semi-)transparent media.

Typically the overall foil thickness is measured in-line by radiographic means. This approach, however, uses hazardous radiation and does not enable the determination of the thickness of the individual layers. This parameter is usually controlled over the weight of the foil material before entering the blown film extrusion line. So far, a reliable control of the final product, however, is only performed off-line. To this end samples pieces are cut out of the multi-layered foils and are analyzed by destructive means, like e.g. microtome microscopy. This approach is time consuming and the results are only available several hours after the production of the foil. Therefore, during this time period the quality of the foil is unknown and it is well possible that the whole intermediate production has to be classified as waste.

http://dx.doi.org/10.5772/53960

The non-destructive and contactless nature of OCT turns this technique an ideal tool for the analysis and quality control of multi-layered foils and other coated structures, as they are often used in the packaging industry. Films with a thickness of only a few microns can easily be resolved with common OCT systems, therefore enabling the analysis of film thickness homogeneity and the detection of impurities [11]. With knowledge on the refractive index of the single layers in the multi-layered foils, even an exact measure of the sample thickness can be provided. With fast OCT systems it is possible to monitor the thickness of the individual layers in moving foils or even in-line [14].

To test the feasibility of OCT to image multi-layered foils moving at different speeds some first off-line tests were performed at the facilities of RECENDT. The experiments were conducted with a portable high speed and high resolution spectral-domain OCT system, similar to the one presented in Figure 1. To meet the requirements of the experiment, the system was equipped with a specially designed single point probing head. A detailed description of the system can be found in [14]. Generally, OCT cross section images are obtained by scanning the probing beam across the sample. In this special application, however, the sample already moves at high speeds in the lateral direction, enabling therefore the acquisition of depth scans at different lateral positions without scanning.

The multi-layered foils were fixed on top of an optical bench and the OCT probe head was moved across the foil at different speeds, ranging from 5 mm/s to 800 mm/s. The probing head was accelerated from its resting position (located on the left or right hand side) and the OCT measurements were performed in the center piece, where the velocity of the probe head was assumed to be constant. Subsequently the probing head was decelerated. The sample had an overall thickness of 290 μm and consisted of 10 different layers. Figure 2 shows a comparison of eight OCT images acquired at different speeds of the probing head, ranging from 5 mm/s to 800 mm/s. The images reveal that even at high speeds of the probing head the image quality allows for a distinction of the individual layers of the foil. The lateral size of the images has a speed dependency and can be calculated over $x = v/f$, where v is the probe head velocity in mm/s and f is the frame rate of the images (20 Hz). The image size in axial direction is 2.57 mm (measured in air).

Subsequently in-line measurements with the same OCT system were performed directly at a blown film extrusion line (Hosokawa Alpine), which is located at the Innovation Headquarter of Borealis Polyolefine in Linz, Austria. With this equipment it is possible to produce multi-layered multi-material foils consisting of up to seven individual layers. Throughout the experiments the overall foil thickness was varied between 30 μm and 200 μm, and the production speed was varied between 266 mm/s and 500 mm/s. The multi-layered foils consisted of layers of different materials (Borclear™ polypropylene, Borshape™ polyethylene, adhesion layer polymer, and EVOH - ethylene vinyl alcohol), where the EVOH layer was sandwiched between two layers of the other materials. Two exemplary OCT images acquired at a production speed of 500 mm/s are presented in Figure 3. Panel a) shows a foil with three layers and an overall thickness of 100 μm. Panel b) depicts two 100 μm thick foils with four layers each. Thickness measurements were performed on all images and showed a good accuracy with the values derived from the microscale measurements on the materials before entering the blown film extrusion line.

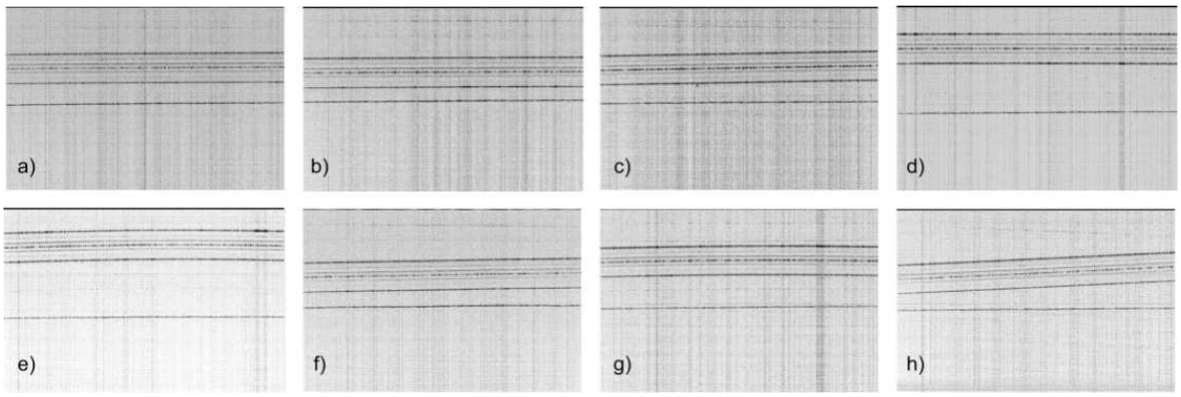

Figure 2. OCT images of multi-layered foils moving at different velocities of a) 5 mm/s; b) 10 mm/s; c) 20 mm/s; d) 50 mm/s; e) 100 mm/s; f) 200 mm/s; g) 300 mm/s; h) 800 mm/s. The image size in axial direction is 2.57 mm (measured in air). In lateral direction the image size has a speed dependency and is a) 0.25 mm; b) 0.5 mm; c) 1 mm; d) 2.5 mm; e) 5 mm; f) 10 mm; g) 15 mm; h) 40 mm [14].

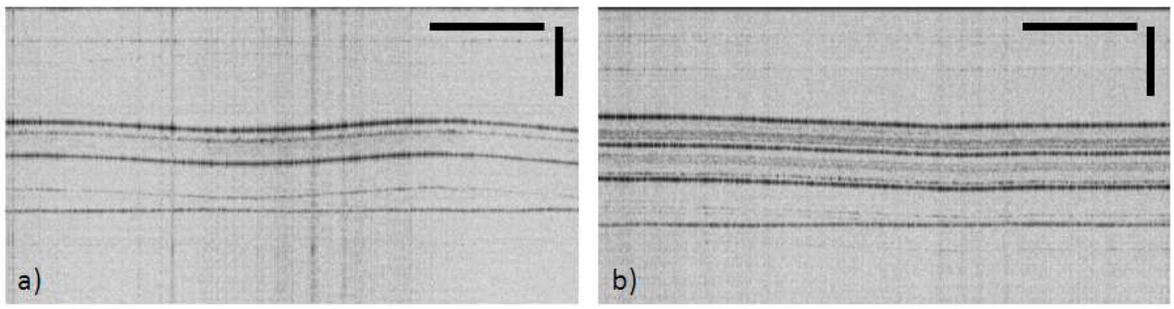

Figure 3. OCT cross-section images acquired in-line at the blow film extruder at a production speed of 500 mm/s; a) single foil with a thickness of 100 µm consisting of three different layers; b) double foil with 100 µm thickness each, consisting of four different layers. The black bars in the lateral and axial dimensions represent 5 mm and 0.3 mm, respectively.

These results showed the applicability of high speed and high resolution optical coherence tomography as a tool for the in-line quality control of multilayered foils. Future work could enhance the system performance towards a real in-line closed loop system. Real time imaging has already been shown with OCT [23], allowing therefore a real time observation of the sample directly during the production process. In this case a dedicated software analysis would provide the possibility to react on variations or inhomogeneities in the thickness of the individual foil layers. Therefore, with such a feed-back loop it should be possible to guarantee the highest quality of the product, to reduce waste, and hence to save resources.

http://dx.doi.org/10.5772/53960

3.2. OCT in plant photonics and for microstructure analysis in food

Until 2000 only a few reports on OCT applications in plant and food sciences were published. Most of them dealt with the layered structure of onions to highlight the applicability and capabilities of the respective OCT devices. The first ones publishing a dedicated report on this topic were Hettinger et al., who proposed optical coherence microscopy (OCM) as a technology for a rapid, in vivo, and non-destructive visualization of plants and plant cells [26]. Since then several general reports on the applicability of OCM/OCT on plant tissue have been published [27–31].

In 2004 Clements et al. reported a study on differences in the hull thickness in four different species of lupin seeds [32]. Lee et al. published work on disease detection in melon seeds [33] and apple leaves [34], proposing the technique as a suitable method for automated screening of viral infection in seeds and leaves, respectively. Detailed studies on the detection of defects, rots, and diseases in onions were published by Meglinski et al. [35] and Ford et al. [36].

An interesting kind of application is the use of OCT to analyze the microstructure of fresh pome fruit. Pome fruit like apples are often stored for several months, and the quality and thickness of the apple skin is one important parameter throughout the storing process [37], for it determines the protection of the apple against liquid and therefore weight loss. To show the ability of optical coherence tomography for the analysis and the control of wax layer thickness we performed OCT imaging sessions on Braeburn apples supplied by the Flanders Centre of Postharvest technology, Belgium. Figure 4 a) shows an OCT cross-section image acquired with an SD-OCT system similar to the one displayed in Figure 1. The image size is 4 x 1.25 mm² and several layers of the paring can clearly be distinguished. Other interesting features for the storage life of apples are the lenticels, which act as a bypass medium for the exchange of gases between the fruit flesh and the ambient. However, also bacteria and funguses can penetrate the fruit through the lenticels. Panels 4 b) and c) show OCT images of lenticels, as acquired with an ultra-high-resolution time-domain-OCT (UHR-TD-OCT) set-up. Panel 4 b) corresponds to a cross section with an image size of 3 x 0.3 mm². A lenticel is clearly visible in the lateral centre of the image, as indicated by the arrow. Panel 4 c) depicts an en-face image of an apple with an image size of 2 x 2 mm², as acquired with a UHR-TD-OCT system, showing the surface of the paring with a lenticel located in the centre. The fragmented appearance of this en-face image is due to the high axial resolution of the OCT set-up, which lies below two microns. Due to the curved shape of the apple, the flat OCT image plane does not fully coincide with the surface of the apple. As a result, in the image the upper left corner yields some bright surface reflections from the paring, whereas the lower part already shows some subsurface pores. Such pores are even better visible in panel 4 d), which has a size of 3 x 3 mm² and was acquired below the surface of another Braeburn apple. Once again, the fragmented appearance of the en-face OCT image is caused by the high axial resolution of the imaging system [38].

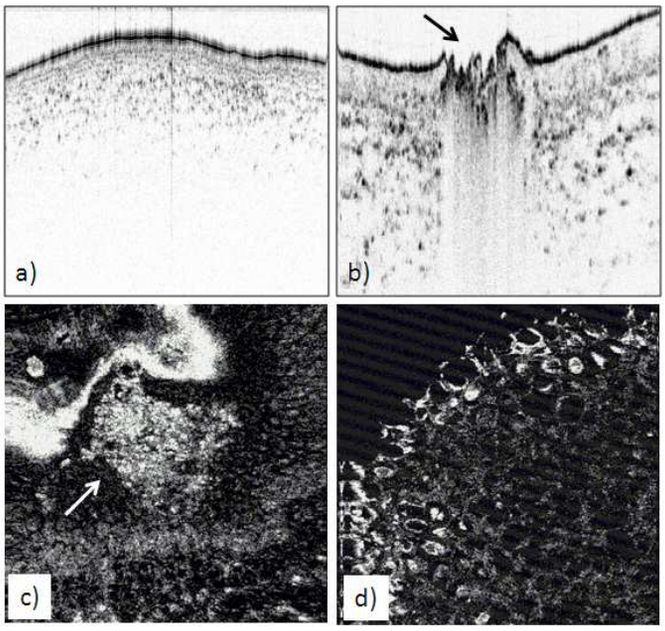

Figure 4. OCT images of Braeburn apples; a) Cross-section image acquired with an SD-OCT system. Image size: 4 x 1.25 mm^2; b) Cross-section image of a lenticel, acquired with a UHR-TD-OCT system. Image size: 3 x 0.3 mm^2; c) En-face OCT image of a lenticel (arrow), acquired with a UHR-TD-OCT set-up. Image size 2 x 2 mm^2; d) en-face OCT image of subsurface pores, acquired with the same system. Image size 3 x 3 mm^2 [38].

Another application of OCT in food science is the analysis of extruded breakfast cereals. In the case of extruded cereals the thickness and homogeneity of sugar coatings, as well as the pore size distribution of the uncoated cereals, are of special interest, since these parameters determine the rehydration properties and the crisp- and crunchiness, respectively. With the aid of OCT it is possible to analyze and monitor these quality indicators during the storage and production processes. Besides a simple analysis of the (sub)surface structures in extruded breakfast cereals it is also possible to study the dynamic rehydration process when immersing extruded breakfast cereals in a liquid like milk. As a specimen for this particular experiment we used coated extruded breakfast cereals provided by NESTEC. The cereals have a spherical shape with a mean diameter of 9 mm and a high surface roughness. They show a high porosity, and as a consequence in the OCT images only the topmost layer is visible. As a liquid we used semi-skimmed milk at room temperature (20°C). The experiments were performed with a Thorlabs TELESTO system. The extruded cereals were fixed on the bottom of a small cylindrical recipient, which was subsequently filled with milk up to approximately 80 % of the height of the cereal balls. 3D OCT images were recorded at a frame rate of 0.25 Hz while the cereal was soaked with milk. Figure 5 shows an OCT volume sequence for one such experiment. The volumes are ordered from a) – d) according to the progress in time during the experiment. Panel a) illustrates the surface of the cereals with no milk visible along the surface. In panel b) some first structural changes can be observed. In panels c) and d) more and more milk becomes apparent along the surface of the cereal ball, resulting in a reformation of the surface morphology. Also a shrinking of the height of the cereal becomes evident, as the structure of the extruded cereal ball is collapsing when being immersed in milk.

http://dx.doi.org/10.5772/53960

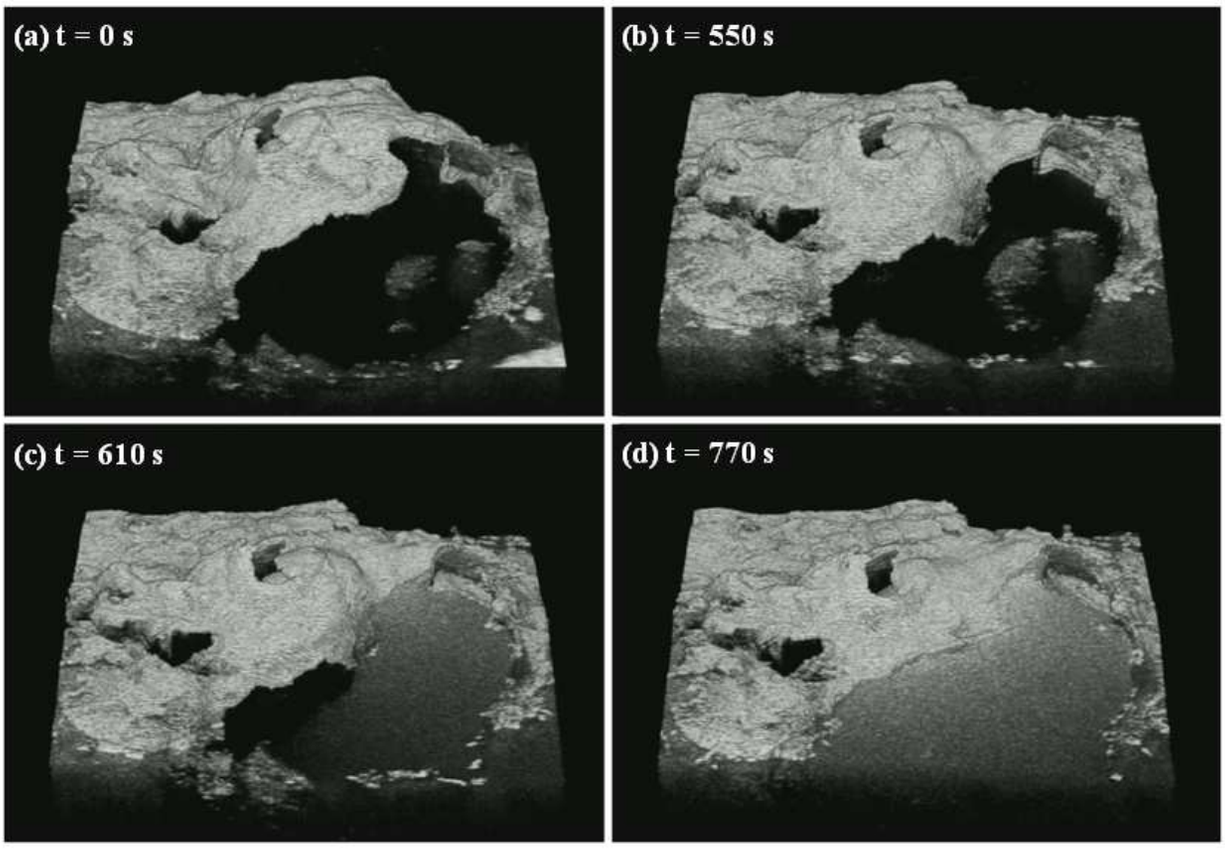

Figure 5. Temporal sequence of 3D OCT images showing the rehydration dynamics of extruded cereals in semi-skimmed milk. The images are ordered from (a) to (d) according to the progress in time. Image size: $4 \times 4 \times 2.5$ mm^3.

The presented studies show the applicability of OCT as a tool in plant photonics and for the microstructure analysis in the food sciences.

3.3. Evaluation of laser induced (sub)surface structures

In many industrial processes there is a need for precise cutting or drilling in the micrometer range. Such cutting or drilling is often performed by ablating matter with the aid of picosecond or femtosecond laser light sources. In some recent publications OCT has been shown as a fast and non-destructive tool to assess the shape and depth of laser induced (sub)surface structures in a variety of different materials. The high sensitivity of OCT thereby allows the imaging of very steep edges, and OCT can also be used to give feedback on the optimum machining parameters. This can be done in a post-processing step, or in situ and in real-time during the machining process in order to give access to dynamic processes.

Webster et al. [39] reported in 2007 the use of light from the same high-power and broadband light source to perform both laser machining in stainless steel and direct observation of the written structures by means of OCT. The laser source was triggered in synchronism with the line scan device in the spectrometer and in this way it was possible to study the ablation dynamics via M-scans. In 2010 Wurm et al. [40] applied OCT to assess the depth and the

width of laser drilled holes in a carbon fiber reinforced composite material by acquiring volume scans with subsequent application of a dedicated software algorithm. In the same year Webster et al. [16] used high speed M-mode OCT to detect relaxation effects between laser pulses in real-time. Furthermore they applied in situ M-mode OCT data to guide the cut into a lead zirconate titanate sample towards a certain target depth through a feedback loop controlling the number of laser pulses. A comparison of two OCT images acquired posterior and ex situ, one without (panel a) and one with (panel b) feedback, is depicted in Figure 6. Also Wiesner et al. [41] reported on in line process control in laser micromaching processes by means of OCT. Recently Goda et al. [42] showed the applicability of high throughput OCT with ~ 91 MHz axial scan rate for real-time monitoring of laser ablation dynamics caused by irradiation of a silicon sample with a mid-infrared laser pulse and a pulse width of 5 ns. With this ultra-high speed imaging system they even managed to acquire whole cross-sections within only 20 μs.

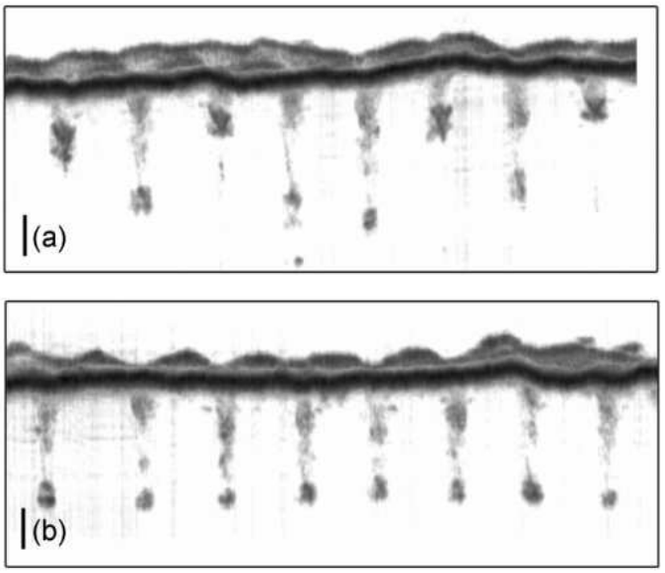

Figure 6. Side view of 3D surface topography of holes cut (a) without and (b) with feedback (B). Volumes above and below the surface correspond to air and steel, respectively. Scale bars are 100 μm (both axes). Reprinted from Paul J.L. Webster, Joe X.Z. Yu, Ben Y.C. Leung, Mitchell D. Anderson, Victor X.D. Yang, James M. Fraser, "*Coherent imaging of morphology change in laser percussion drilling*," Opt.Lett. 2010, *35*, 646-648, with permission from the Optical Society of America © 2010[16].

These recent studies highlight the high potential of OCT for the analysis of dynamic effects in laser micromachining and as a feedback tool to control the depth of the written structures.

3.4. Characterization of tablet coatings

A very recent application of OCT is the characterization of tablet coatings. Film coating is a widely used unit operation in the pharmaceutical industry for solid dosage form manufacturing, fulfilling different purposes ranging from aesthetic and trade marking issues to functionalized coatings, for taste masking, improved product stability, shelf life increase or

http://dx.doi.org/10.5772/53960

controlled release of the active pharmaceutical ingredient (API). In addition, functional coatings allow formulators to alter the initial drug release kinetics to be pH dependent by making it resistant to gastric juice through enteric coatings, i.e., controlled-release formulations. Alternatively, it is possible to retard the onset of the drug release by controlling the dissolution rate via semi-permeable membranes. Furthermore, active ingredients may be incorporated in the film layer [15].

Although coating processes have been used for many decades, there are still serious challenges, as there is a lack of understanding of how material and operating parameters impact product quality. Different problems can arise, such as picking (i.e., part of the film coating is pulled off one tablet and is deposited on another), twinning (i.e., two or more of the tablet cores are stuck together), orange peel (i.e., a roughened film due to spray drying), bridging (e.g., film coating lifts up out of the tablet logo), cracking (e.g., due to internal stresses in the film), coating inhomogeneity, and film thickness variations within a batch due to poor process and equipment design.

At the moment, there are many Process Analytical Technology (PAT) tools available, providing information about physicochemical product properties, ranging from the chemical composition or even the quantitative determination of the film coating thickness. Here, spectroscopic techniques like NIR and Raman were already demonstrated to be powerful tools for offline product characterization, as well as for in-line process monitoring. Combined with multivariate data analysis (MVDA), these methods enable for quantitative and non-invasive process monitoring and fulfill also most of the needs for robust and fast measurements.

However, these systems are often applied for characterizing the whole batch, where only averaged values for the film thickness are available from a moving tablet bed in a drum coater for instance. This value is a very good indicator for the overall process status, but provides little information about variations between single tablets, such as coating morphology and homogeneity. Even though well established quality control parameters, such as weight gain, indicate coating properties within specifications for the whole batch, no general conclusion can be drawn for the variation from tablet-to-tablet within a batch or the overall coating homogeneity of a single tablet. Hence, there is an increasing need for novel techniques, enabling accurate spatially (laterally and axially) resolved characterization of the coating. A comprehensive review on potential techniques fulfilling these requirements was given by Zeitler and Gladden [43], where X-ray computed microtomography (XμCT), magnetic resonance imaging (MRI), imaging at terahertz frequencies and OCT were evaluated and discussed for their informative value. These techniques can be considered as tomographic, i.e., allowing for a non-destructive three-dimensional investigation of dosage forms. In contrast to MRI and XμCT, OCT and terahertz pulsed imaging (TPI) are quite similar techniques and currently the only optical techniques used for non-destructive characterization of tablet coatings. Other studies on the application of OCT for the characterization of tablet coatings were published by Juuti et al. [44], Mauritz et al. [45], Zhong et al. [46] and Koller et al. [15].

In the work published by Koller et al. [15] OCT was utilized for a quantitative characterization of pharmaceutical tablet film coatings, sampled at different stages of an industrial drum spray coating process. OCT was selected from the above mentioned techniques due to its high axial and lateral resolution, which allows the investigation of very thin layers, due to its contact-free measurement properties, which is very important for curved surfaces and due to the high data acquisition rates for fast product characterization. The investigated tablets (round, biconvex Thrombo ASS 50 mg with an enteric coating of Eudragit® L30D-55) were sampled at 15 different stages (Lots) of the coating process, comprising tablets with a coating thickness ranging from uncoated to a target coating thickness of about 70 μm. The spray coating process was performed on a batch of approximately 1.2 million tablets using a BTC 400 perforated drum coater (L.B. Bohle Maschinen + Verfahren GmbH, Ennigerloh, Germany). From each sample set, five tablets were analyzed offline to get the statistical variation of the coating process. Besides the investigation with OCT in terms of layer thickness und homogeneity, tablet weight gain and tablet diameters were determined on a single-tablet level. Scanning electron microscopy (SEM) was applied on cracked tablets for referencing the coating thickness obtained with OCT.

Figure 7 shows a comparison between tablets of Lots 1, 7, 8, 9, 10, 11, 12, 14 and 15, as acquired with a spectral-domain OCT system similar to the one depicted in Figure 1. Details on the OCT system are available in Koller et al. [15]. The image size is 4.3 x 0.36 mm² with a resolution of 4.3 μm and < 4 μm in lateral and axial direction, respectively. The image acquisition rate was 1.5 images/s for the B-Scans (including display on screen). Due to the different resolutions, the images show different scales in lateral and axial direction. The illustrated coating thickness is represented by the optical path length, which is a function of the refractive index of the coating material ($n_{Eudragit} \approx 1.48$). Thus, an accurate determination of the coating thickness with the SD-OCT system is possible, as long as an appropriate contrast at the interfaces of the coating allows a clear discrimination between materials. The snapshots in Figure 7 are ordered from top to bottom according to the progress in the coating process, with Lot 1 representing a non-coated and Lot 15 a fully coated tablet. The increase in the coating thickness is clearly evident in the images. This highlights the potential of OCT, as even very thin layers at the beginning of the coating process can be analyzed. The arrows indicate defects in the coating or the underlying bulk material. These may result from inclusions of air during the coating process or density variations leading to increased light scattering. The features visible below the coating are caused by photons back-scattered from the substrate material. When using an OCT system working at longer wavelengths (e.g. 1300 nm) a deeper penetration into the substrate should be possible, however at the cost of a lower axial resolution.

With the results from the studies performed so far OCT turned out to be a very powerful tool for the characterization of tablet coatings.

http://dx.doi.org/10.5772/53960

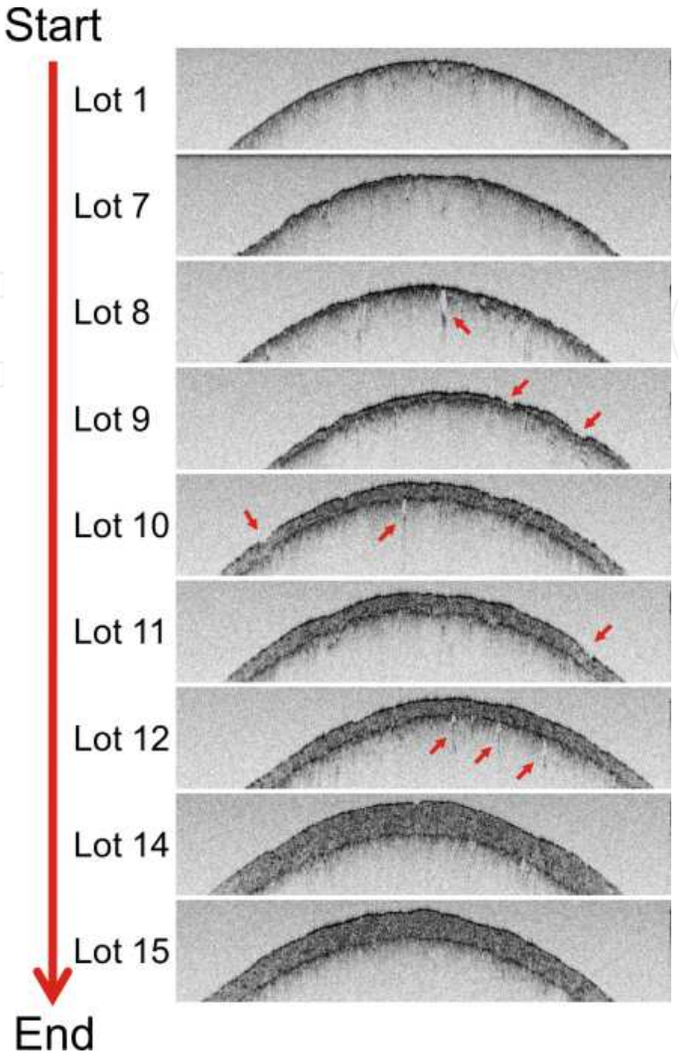

Figure 7. SD-OCT B-Scan images of tablets from different stages of the coating process. The image size is 4.3 x 0.36 mm^2 (measured in air) with a resolution of 4.3 µm and <4 µm in lateral and axial direction, respectively. Reprinted from Koller, D.M.; Hannesschläger, G.; Leitner, M.; Khinast, J.G. Non-destructive analysis of tablet coatings with optical coherence tomography. *European Journal of Pharmaceutical Sciences* 2011, *44*, 142–148, with permission from Elsevier © 2011 [15].

3.5. Evaluation of structural changes in materials

Many materials undergo structural changes during the production process or during their lifecycle. Examples include hardening, cooling or heating phases, or changes due to mechanical load or stress. OCT, and especially the functional extension of polarization sensitive OCT (PS-OCT), is a fast, fully contactless, and non-destructive approach to monitor and evaluate such processes. PS-OCT gives access to the birefringence of the sample and additional measurements of full Stokes vectors and Mueller matrices, as well as the simultaneous determination of intensity, retardation and orientation of the optical axes have been reported. A review on PS-OCT was published by de Boer et al. [47]. Reports on applications of PS-OCT in the field of NDT have been published, among others, in [12,13,21,48–55].

For a thorough review on applications of PS-OCT in the field of NDT the reader is referred to Chapter by Dr. Bettina Heise.

3.6. Other applications of OCT in NDTE

Besides the applications introduced so far, over the past few years OCT has also been applied to a vast variety of different samples and materials. For example several groups focused their efforts on the characterization of artwork, with a recent review on this topic having been published by Targowski et al. [22].

Especially the group around Myllylä in Oulu, Finland, is heavily engaged in the application of OCT for NDT. Over the last years they have applied OCT for the characterization of paper [56–59], printed electronics circuits [19,60] and also used OCT as a method for the characterization of wettability [61].

OCT can also be used to detect forgery in ancient jade [62] or banknotes [63], or the security thread in valuable documents [64]. A similar application is the one reported by Ju et al. for the evaluation and identification of pearls [65].

Furthermore, over the past few years OCT has been introduced as a tool to characterize and investigate samples, like e.g., organic solar cells [17], aerospace materials [66], light emitting diodes [67], periodically poled ferroelectrics [68], wet pad surfaces in chemical mechanical polishing processes [69], embedded micro channels in alumina ceramics [70], and even to study boiling phenomena [71].

4. Summary and outlook

In this chapter some applications of optical coherence tomography in non-destructive testing were presented and discussed. After an introduction to the technique of OCT and some considerations related to its use in non-destructive testing, a brief overview on the development of applications of OCT in the field of NDT was given. Special emphasis was paid to recent reports on topics like the characterization of multi-layered foils, studies on plant photonics and the microstructure in foods, the characterization of laser induced (sub)surface structures, and the determination of coating thickness in pharmaceutical tablets. In the end a brief overview on other NDT-related applications of OCT was provided.

With respect to the strong increase in the number of research groups working on OCT applications outside the field of biomedicine it is to be expected that the number of publications will rise drastically within the next few years. New applications for lab based and desktop OCT devices will be found, helping to better understand a wide variety of material systems and processes. On the other hand, so far the number of reports on the use of OCT in industrial environments and for the in situ and real-time monitoring of industrial processes is still scarce. However, some first and very promising reports pointing into this direction were reviewed in this chapter, triggering the demand for faster and more robust OCT devices in the future.

http://dx.doi.org/10.5772/53960

Acknowledgements

Financial support is gratefully acknowledged from the European Union (project FP7-226783 – InsideFood; The opinions expressed in this document do by no means reflect the official opinion of the European Union or its representatives), the „K-Project for Non-Destructive Testing and Tomography" supported by the COMET-program of the Austrian Research Promotion Agency (FFG), Grant No. 820492, the European Regional Development Fund (EFRE) in the framework of the EU-program REGIO 13, and the federal state of Upper Austria is gratefully acknowledged.

Author details

Alexandra Nemeth, Günther Hannesschläger, Elisabeth Leiss-Holzinger,
Karin Wiesauer and Michael Leitner

*Address all correspondence to: michael.leitner@recendt.at

Research Center for Non-Destructive Testing GmbH, Linz, Austria

References

[1] Huang, D.; Swanson, E.A.; Lin, C.P.; Schuman, J.S.; Stinson, W.G.; Chang, W.; Hee; Flotte, T.; Gregory, K.; Puliafito, C.A.; et al. Optical coherence tomography. Science 1991, 254, 1178–1181.

[2] Drexler, W.; Morgner, U.; Kärtner, F.X.; Pitris, C.; Boppart, S.A.; Li, X.D.; Ippen, E.P.; Fujimoto, J.G. In vivo ultrahigh-resolution optical coherence tomography. Opt. Lett. 1999, 24, 1221–1223.

[3] Colston, B.; Sathyam, U.; DaSilva, L.; Everett, M.; Stroeve, P.; Otis, L. Dental OCT. Opt. Express 1998, 3, 230–238.

[4] Podoleanu, A.; Rogers, J.; Jackson, D.; Dunne, S. Three dimensional OCT images from retina and skin. Opt. Express 2000, 7, 292–298.

[5] Jang, I.-K.; Bouma, B.E.; Kang, D.-H.; Park, S.-J.; Park, S.-W.; Seung, K.-B.; Choi, K.-B.; Shishkov, M.; Schlendorf, K.; Pomerantsev, E.; et al. Visualization of coronary atherosclerotic plaques in patients using optical coherence tomography: comparison with intravascular ultrasound. Journal of the American College of Cardiology 2002, 39, 604–609.

[6] Jenkins, M.W.; Duke, A.R.; Gu, S.; Doughman, Y.; Chiel, H.J.; Fujioka, H.; Watanabe, M.; Jansen, E.D.; Rollins, A.M. Optical pacing of the embryonic heart. Nat Photon 2010, 4, 623–626.

[7] Swanson, E.A.; Hee, M.R.; Tearney, G.J.; Fujimoto, J.G. Application of optical coherence tomography in nondestructive evaluation of material microstructure. In Lasers and Electro-Optics, 1996. CLEO '96., 1996, pp. 326–327.

[8] Bashkansky, M.; Battle, P.R.; Duncan, M.D.; Kahn, M.; Reintjes, J. Subsurface Defect Detection in Ceramics Using an Optical Gated Scatter Reflectometer. Journal of the American Ceramic Society 1996, 79, 1397–1400.

[9] Bashkansky, M.; Duncan, M.D.; Kahn, M.; Lewis III, D.; Reintjes, J. Subsurface defect detection in ceramics by high-speed high-resolution optical coherent tomography. Opt. Lett. 1997, 22, 61–63.

[10] Duncan, M.; Bashkansky, M.; Reintjes, J. Subsurface defect detection in materialsusing optical coherence tomography. Opt. Express 1998, 2, 540–545.

[11] Wiesauer, K.; Pircher, M.; Götzinger, E.; Bauer, S.; Engelke, R.; Ahrens, G.; Grützner, G.; Hitzenberger, C.; Stifter, D. En-face scanning optical coherence tomography with ultra-high resolution for material investigation. Opt. Express 2005, 13, 1015–1024.

[12] Wiesauer, K.; Pircher, M.; Goetzinger, E.; Hitzenberger, C.K.; Engelke, R.; Ahrens, G.; Gruetzner, G.; Stifter, D. Transversal ultrahigh-resolution polarization-sensitive optical coherence tomography for strain mapping in materials. Opt. Express 2006, 14, 5945–5953.

[13] Stifter, D. Beyond Biomedicine: A Review of Alternative Applications And Developments For Optical Coherence Tomography. Applied Physics B 2007, 88, 337–357.

[14] Hannesschläger, G.; Nemeth, A.; Hofer, C.; Goetzloff, C.; Reussner, J.; Wiesauer, K.; Leitner, M. Optical coherence tomography as a tool for non destructive quality control of multi-layered foils. In Proceedings of the 6th NDT in Progress 2011, International Workshop of NDT Experts, Prag, 10.09-12.09.2011, 2011, pp. Paper 7.

[15] Koller, D.M.; Hannesschläger, G.; Leitner, M.; Khinast, J.G. Non-destructive analysis of tablet coatings with optical coherence tomography. European Journal of Pharmaceutical Sciences 2011, 44, 142–148.

[16] Webster, P.J.L.; Yu, J.X.Z.; Leung, B.Y.C.; Anderson, M.D.; Yang, V.X.D.; Fraser, J.M. In situ 24 kHz coherent imaging of morphology change in laser percussion drilling. Opt. Lett 2010, 35, 646-648.

[17] Thrane, L.; Jørgensen, T.M.; Jørgensen, M.; Krebs, F.C. Application of optical coherence tomography (OCT) as a 3-dimensional imaging technique for roll-to-roll coated polymer solar cells. Solar Energy Materials and Solar Cells 2012, 97, 181–185.

[18] Alarousu, E.; Krehut, L.; Prykäri, T.; Myllylä, R. Study on the use of optical coherence tomography in measurements of paper properties. Measurement Science and Technology 2005, 16, 1131.

[19] Czajkowski, J.; Prykäri, T.; Alarousu, E.; Palosaari, J.; Myllylä, R. Optical coherence tomography as a method of quality inspection for printed electronics products. Optical Review 2010, 17, 257–262.

[20] Stifter, D.; Leiss-Holzinger, E.; Major, Z.; Baumann, B.; Pircher, M.; Götzinger, E.; Hitzenberger, C.K.; Heise, B. Dynamic optical studies in materials testing with spectral-domain polarization-sensitive optical coherence tomography. Optics Express 2010, 18, 25712–25725.

[21] Targowski, P.; Iwanicka, M. Optical Coherence Tomography: its role in the non-invasive structural examination and conservation of cultural heritage objects - a review. Applied Physics A: Materials Science & Processing 2012, 106, 265–277.

[22] van der Jeught, S.; Bradu, A.; Podoleanu, A.G. Real-time resampling in Fourier domain optical coherence tomography using a graphics processing unit. J. Biomed. Opt. 2010, 15, 30511–3.

[23] Chen, Z.; Milner, T.E.; Dave, D.; Nelson, J.S. Optical Doppler tomographic imaging of fluid flow velocity in highly scattering media. Opt. Lett. 1997, 22, 64–66.

[24] Pircher, M.; Götzinger, E.; Leitgeb, R.; Fercher, A.; Hitzenberger, C. Measurement and imaging of water concentration in human cornea with differential absorption optical coherence tomography. Opt. Express 2003, 11, 2190–2197.

[25] Hettinger, J.W.; La Mattozzi, M.P. de; Myers, W.R.; Williams, M.E.; Reeves, A.; Parsons, R.L.; Haskell, R.C.; Petersen, D.C.; Wang, R.; Medford, J.I. Optical Coherence Microscopy. A Technology for Rapid, in Vivo, Non-Destructive Visualization of Plants and Plant Cells. Plant Physiology 2000, 123, 3–16.

[26] Reeves, A.; Parsons, R.L.; Hettinger, J.W.; Medford, J.I. In vivo three-dimensional imaging of plants with optical coherence microscopy. Journal of Microscopy 2002, 208, 177-189.

[27] Sapozhnikova, V.V.; Kamenskii, V.A.; Kuranov, R.V. Visualization of Plant Tissues by Optical Coherence Tomography. Russian Journal of Plant Physiology 2003, 50, 282–286.

[28] Kutis, I.S.; Sapozhnikova, V.V.; Kuranov, R.V.; Kamenskii, V.A. Study of the Morphological and Functional State of Higher Plant Tissues by Optical Coherence Microscopy and Optical Coherence Tomography. Russian Journal of Plant Physiology 2005, 52, 559–564.

[29] Boccara, M.; Schwartz, W.; Guiot, E.; Vidal, G.; Paepe, R. de; Dubois, A.; Boccara, A.-C. Early chloroplastic alterations analysed by optical coherence tomography during a harpin-induced hypersensitive response. The Plant Journal 2007, 50, 338–346.

[30] Loeb, G.; Barton, J.K. Imaging botanical subjects with optical coherence tomography: a feasibility study, 2008.

[31] Clements, J.C.; Zvyagin, A.V.; Silva, K.K.M.B.D.; Wanner, T.; Sampson, D.D.; Cowling, W.A. Optical coherence tomography as a novel tool for non-destructive measurement of the hull thickness of lupin seeds. Plant Breeding 2004, 123, 266-270.

[32] Lee, C.; Lee, S.-Y.; Kim, J.-Y.; Jung, H.-Y.; Kim, J. Optical Sensing Method for Screening Disease in Melon Seeds by Using Optical Coherence Tomography. Sensors 2011, 11, 9467-9477.

[33] Lee, C.-H.; Lee, S.-Y.; Jung, H.-Y.; Kim, J.-H. The Application of Optical Coherence Tomography in the Diagnosis of Marssonina Blotch in Apple Leaves. J. Opt. Soc. Korea 2012, 16, 133-140.

[34] Meglinski, I.; Buranachai, C.; Terry, L. Plant photonics: application of optical coherence tomography to monitor defects and rots in onion. Laser Physics Letters 2010, 7, 307-310.

[35] Ford, H.D.; Tatam, R.P.; Landahl, S.; Terry, L.A. Investigation of disease in stored onions using optical coherence tomography. In IV International Conference Postharvest Unlimited 2011, pp. 247–254.

[36] Veraverbeke, E.A.; van Bruaene, N.; van Oostveldt, P.; Nicolaï, B.M. Non destructive analysis of the wax layer of apple Malus domestica by means of confocal laser scanning microscopy. Planta 2001, 213, 525–533.

[37] Leitner, M.; Hannesschläger, G.; Saghy, A.; Nemeth, A.; Chassagne-Berces, S.; Chanvrier, H.; Herremans, E.; Verlinden, B. Optical coherence tomography for quality control and microstructure analysis in food. In ICEF Athens, 22.-26.05.2011, 2011.

[38] Webster, P.J.L.; Muller, M.S.; Fraser, J.M. High speed in situ depth profiling of ultrafast micromachining. Opt. Express 2007, 15, 14967-14972.

[39] Wurm, M.; Hofer, C.; Traxler, H.; Zabernig, A.; Harrer, B. Vermessung der Laserbohrungen in faserverstärktem Graphit mittels Optischer Kohärenztomographie. In Industrielle Computertomographie, Wels, 27.-29.09.2010, 2010, pp. 133–140.

[40] Wiesner, M.; Ihlemann, J.; Muller, H.H.; Lankenau, E.; Huttmann, G. Optical coherence tomography for process control of laser micromachining. Rev. Sci. Instrum. 2010, 81, 33705–7.

[41] Goda, K.; Fard, A.; Malik, O.; Fu, G.; Quach, A.; Jalali, B. High-throughput optical coherence tomography at 800 nm. Opt. Express 2012, 20, 19612–19617.

[42] Zeitler, J.A.; Gladden, L.F. In-vitro tomography and non-destructive imaging at depth of pharmaceutical solid dosage forms: Special Issue: Solid State and Solid Dosage Forms. European Journal of Pharmaceutics and Biopharmaceutics 2009, 71, 2–22.

[43] Juuti, M.; Tuononen, H.; Prykäri, T.; Kontturi, V.; Kuosmanen, M.; Alarousu, E.; Ketolainen, J.; Myllylä, R.; Peiponen, K. Optical and terahertz measurement techniques for flat-faced pharmaceutical tablets: a case study of gloss, surface roughness and

bulk properties of starch acetate tablets. Measurement Science and Technology 2009, 20, 15301.

[44] Mauritz, J.M.A.; Morrisby, R.S.; Hutton, R.S.; Legge, C.H.; Kaminski, C.F. Imaging pharmaceutical tablets with optical coherence tomography. J. Pharm. Sci. 2010, 99, 385–391.

[45] Zhong, S.; Shen, Y.-C.; Ho, L.; May, R.K.; Zeitler, J.A.; Evans, M.; Taday, P.F.; Pepper, M.; Rades, T.; Gordon, K.C.; et al. Non-destructive quantification of pharmaceutical tablet coatings using terahertz pulsed imaging and optical coherence tomography. Optics and Lasers in Engineering 2011, 49, 361–365.

[46] Boer, J.F. de; Milner, T.E. Review of polarization sensitive optical coherence tomography and Stokes vector determination. J. Biomed. Opt. 2002, 7, 359–371.

[47] Oh, J.-T.; Kim, S.-W. Polarization-sensitive optical coherence tomography for photoelasticity testing of glass/epoxy composites. Opt. Express 2003, 11, 1669–1676.

[48] Stifter, D.; Burgholzer, P.; Höglinger, O.; Götzinger, E.; Hitzenberger, C.K. Polarisation-sensitive optical coherence tomography for material characterisation and strain-field mapping. Applied Physics A: Materials Science & Processing 2003, 76, 947–951.

[49] Wiesauer, K.; Dufau, A.D.S.; Götzinger, E.; Pircher, M.; Hitzenberger, C.K.; Stifter, D. Non-destructive quantification of internal stress in polymer materials by polarisation sensitive optical coherence tomography. Acta Materialia 2005, 53, 2785–2791.

[50] Wiesauer, K.; Pircher, M.; Götzinger, E.; Hitzenberger, C.K.; Oster, R.; Stifter, D. Investigation of glass–fibre reinforced polymers by polarisation-sensitive, ultra-high resolution optical coherence tomography: Internal structures, defects and stress. Composites Science and Technology 2007, 67, 3051–3058.

[51] Engelke, R.; Ahrens, G.; Arndt-Staufenbiehl, N.; Kopetz, S.; Wiesauer, K.; Löchel, B.; Schröder, H.; Kastner, J.; Neyer, A.; Stifter, D.; et al. Investigations on possibilities of inline inspection of high aspect ratio microstructures. Microsystem Technologies 2007, 13, 319–325.

[52] Wiesauer, K.; Pircher, M.; Gtzinger, E.; Hitzenberger, C.K.; Engelke, R.; Grtzner, G.; Ahrens, G.; Oster, R.; Stifter, D. Measurement of structure and strain by transversal ultra-high resolution polarisation-sensitive optical coherence tomography. Insight - Non-Destructive Testing and Condition Monitoring 2007, 49, 275–278.

[53] Heise, B.; Wiesauer, K.; Götzinger, E.; Pircher, M.; Hitzenberger, C.K.; Engelke, R.; Ahrens, G.; Grützner, G.; Stifter, D. Spatially Resolved Stress Measurements in Materials With Polarisation-Sensitive Optical Coherence Tomography: Image Acquisition and Processing Aspects. Strain 2010, 46, 61–68.

[54] Leiss-Holzinger, E.; Cakmak, U.D.; Heise, B.; Bouchot, J.L.; Klement, E.P.; Leitner, M.; Stifter, D.; Major, Z. Evaluation of structural change and local strain distribution in polymers comparatively imaged by FFSA and OCT techniques. eXPRESS Polymer Letters 2012, 6, 249–256.

[55] Alarousu, E.; Krehut, L.; Prykäri, T.; Myllylä, R. Study on the use of optical coherence tomography in measurements of paper properties. Measurement Science and Technology 2005, 16, 1131.

[56] Fabritius, T.; Myllylä, R. Liquid sorption investigation of porous media by optical coherence tomography. Journal of Physics D: Applied Physics 2006, 39, 4668.

[57] Fabritius, T.; Myllylä, R. Investigation of swelling behaviour in strongly scattering porous media using optical coherence tomography. Journal of Physics D: Applied Physics 2006, 39, 2609.

[58] Prykäri, T.; Czajkowski, J.; Alarousu, E.; Myllylä, R. Optical coherence tomography as an accurate inspection and quality evaluation technique in paper industry. Optical Review 2010, 17, 218–222.

[59] Czajkowski, J.; Fabritius, T.; Ulański, J.; Marszałek, T.; Gazicki-Lipman, M.; Nosal, A.; Śliż, R.; Alarousu, E.; Prykäri, T.; Myllylä, R.; et al. Ultra-high resolution optical coherence tomography for encapsulation quality inspection. Applied Physics B: Lasers and Optics 2011, 105, 649–657.

[60] Fabritius, T.; Myllylä, R.; Makita, S.; Yasuno, Y. Wettability characterization method based on optical coherence tomography imaging. Opt. Express 2010, 18, 22859–22866.

[61] Chang, S.; Mao, Y.; Chang, G.; Flueraru, C. Jade detection and analysis based on optical coherence tomography images. Optical Engineering 2010, 49, 63602.

[62] Choi, W.-J.; Min, G.-H.; Lee, B.-H.; Eom, J.-H.; Kim, J.-W. Counterfeit Detection Using Characterization of Safety Feature on Banknote with Full-field Optical Coherence Tomography. J. Opt. Soc. Korea 2010, 14, 316–320.

[63] Fujiwara, K.; Matoba, O. High-speed cross-sectional imaging of valuable documents using common-path swept-source optical coherence tomography. Appl. Opt. 2011, 50, H165.

[64] Ju, M.J.; Lee, S.J.; Min, E.J.; Kim, Y.; Kim, H.Y.; Lee, B.H. Evaluating and identifying pearls and their nuclei by using optical coherence tomography. Opt. Express 2010, 18, 13468–13477.

[65] Liu, P.; Groves, R.M.; Benedictus, R. Quality assessment of aerospace materials with optical coherence tomography 2012, 84300I.

[66] Cho, N.H.; Jung, U.; Kim, S.; Kim, J. Non-Destructive Inspection Methods for LEDs Using Real-Time Displaying Optical Coherence Tomography. Sensors 2012, 12, 10395-10406.

[67] Pei, S.-C.; Ho, T.-S.; Tsai, C.-C.; Chen, T.-H.; Ho, Y.; Huang, P.-L.; Kung, A.H.; Huang, S.-L. Non-invasive characterization of the domain boundary and structure properties of periodically poled ferroelectrics. Opt. Express 2011, 19, 7153–7160.

[68] Choi, W.J.; Jung, S.P.; Shin, J.G.; Yang, D.; Lee, B.H. Characterization of wet pad surface in chemical mechanical polishing (CMP) process with full-field optical coherence tomography (FF-OCT). Opt. Express 2011, 19, 13343–13350.

[69] Su, R.; Kirillin, M.; Ekberg, P.; Roos, A.; Sergeeva, E.; Mattsson, L. Optical coherence tomography for quality assessment of embedded microchannels in alumina ceramic. Opt. Express 2012, 20, 4603–4618.

[70] Meissner, S.; Herold, J.; Kirsten, L.; Schneider, C.; Koch, E. 3D optical coherence tomography as new tool for microscopic investigations of nucleate boiling on heated surfaces. International Journal of Heat and Mass Transfer 2012, 55, 5565–5569.

IntechOpen